

## Recruitment modelling for Antarctic krill (*Euphausia superba*) stock assessments considering the recurrence of years with low recruitment

C. Pavez<sup>1</sup>, S. Wotherspoon<sup>1,2</sup>, D. Maschette<sup>1,2</sup>, K. Reid<sup>1,3</sup> and K.M. Swadling<sup>1</sup>

<sup>1</sup> Fisheries and Aquaculture Centre, Institute for Marine and Antarctic Studies  
University of Tasmania  
Hobart, 7001, Tasmania  
Australia

<sup>2</sup> Department of Climate Change, Energy, the Environment and Water  
Australian Antarctic Division  
203 Channel Highway  
Kingston, 7050, Tasmania  
Australia  
Email: [Simon.Wotherspoon@aad.gov.au](mailto:Simon.Wotherspoon@aad.gov.au)

<sup>3</sup> Ross Analytics PTY LTD  
1 Lynden Road, Bonnet Hill  
Tasmania 7053  
Australia

### Abstract

Antarctic krill (*Euphausia superba*) is a keystone species in the Southern Ocean food web, and, as such, it is crucial to effectively manage the krill fishery to ensure its long-term sustainability. Setting precautionary catch limits for krill relies on sampling and population modelling. Krill stock projections are developed with the generalised yield model (GYM), which provides an assessment for stock status under current harvesting scenarios and various levels of uncertainties. One of the fundamental components of the GYM is the simulation of recruitment. De la Mare (1994) presents a proportional recruitment model for estimating krill recruitment based on length-frequency distributions collected from field surveys. The de la Mare (1994) function uses estimates of the mean and variance of proportional recruitment from survey data to determine the scaling of natural mortality and the distribution of random recruits that reproduce the observed mean and variance estimates. Here we evaluated de la Mare's (1994) proportional recruitment function and found that for large variations in recruitment the function does not accurately reproduce the observed mean proportion of recruits and its variance. The deficiencies within the de la Mare (1994) function were reviewed and two alternative methods were provided, which can support a wider range of values and possible scenarios, such as years of extremely low recruitment.

### Résumé

Le krill antarctique (*Euphausia superba*) constitue la clef de voûte du réseau trophique de l'océan Austral. Il est donc essentiel d'en assurer la durabilité à long terme à travers une gestion efficace de la pêcherie de krill. La définition des limites de capture de précaution pour le krill repose sur l'échantillonnage et la modélisation de la population. Les projections du stock de krill sont élaborées à l'aide du modèle de rendement généralisé (GYM), qui fournit une évaluation de l'état du stock dans les scénarios de capture actuels et avec différents niveaux d'incertitudes. L'un des éléments fondamentaux du GYM est la simulation du recrutement. De la Mare (1994) présente un modèle de recrutement proportionnel permettant l'estimation du recrutement du krill d'après les distributions des fréquences de taille collectées lors de campagnes de terrain. La fonction de de la Mare (1994) utilise des estimations de la moyenne et de la variance du recrutement proportionnel effectuées à partir de données issues de campagnes d'évaluation afin de déterminer l'échelle de la mortalité naturelle et la répartition géographique des recrues

aléatoires qui reproduisent les estimations de la moyenne et de la variance. Cette étude a évalué la fonction de recrutement proportionnel de De la Mare (1994) et déterminé que lorsque d'importantes variations existent dans le recrutement, la fonction ne reproduit pas correctement la proportion moyenne observée des recrues et sa variance. À la suite de l'examen des déficiences de la fonction de De la Mare (1994), deux méthodes de remplacement sont fournies, permettant de soutenir un éventail de valeurs plus large et de possibles scénarios, telles que des années de recrutement extrêmement faible.

### Резюме

Антарктический криль (*Euphausia superba*) – ключевой вид кормовой сети Южного океана, и поэтому очень важно эффективно управлять промыслом криля, чтобы обеспечить его долгосрочную устойчивость. Установление предохранительных ограничений на вылов криля основывается на отборе проб и моделировании популяций. Прогнозы запасов криля разрабатываются с помощью обобщенной модели вылова (GYM), которая позволяет оценить состояние запасов при текущих сценариях промысла и различных уровнях неопределенности. Одним из основополагающих компонентов GYM является моделирование пополнения. Де ла Маре (1994) предлагает модель пропорционального пополнения для оценки пополнения криля на основе распределений длины и частоты, полученных в результате промысловых съемок. Функция Де ла Маре (1994) основывается на оценках среднего и дисперсии пропорционального пополнения по данным съемок для определения масштаба естественной смертности и распределения случайных пополнений, которые отражают наблюдаемые оценки среднего пополнения и его дисперсии. В данной работе мы проанализировали функцию пропорционального пополнения Де ла Маре (1994) и обнаружили, что при высоких перепадах в пополнении данная функция неточно воспроизводит наблюдаемую среднюю долю пополнения и ее дисперсию. Были рассмотрены недостатки функции Де ла Маре (1994) и предложены два альтернативных метода, которые могут учитывать более широкий диапазон значений и возможные сценарии, например, годы с крайне низким уровнем пополнения.

### Resumen

El kril antártico (*Euphausia superba*) es una especie fundamental en la cadena alimentaria del océano Austral y, como tal, es importante ordenar la pesquería de kril de manera eficaz para garantizar su sostenibilidad a largo plazo. El establecimiento de límites de captura precautorios para el kril se basa en muestreos y modelado de poblaciones. Las proyecciones de los stocks de kril se desarrollan con el modelo generalizado de rendimiento (GYM), que proporciona una evaluación del estado de los stocks bajo escenarios actuales de cosecha y varios niveles de incertidumbre. Uno de los componentes fundamentales del GYM es la simulación de reclutamiento. De la Mare (1994) presenta un modelo proporcional de reclutamiento para estimar el reclutamiento de kril basado en distribuciones de la frecuencia de tallas recopiladas de prospecciones de campo. La función de De la Mare (1994) utiliza estimaciones de la media y la varianza del reclutamiento proporcional a partir de datos de prospecciones para determinar la escala de la mortalidad natural y la distribución de reclutas aleatorios que reproducen las estimaciones observadas de la media y la varianza. En el presente estudio evalúa la función de reclutamiento proporcional de De la Mare (1994) y se puede observar que, en el caso de grandes variaciones en el reclutamiento, la función no reproduce con precisión la proporción media observada de reclutas y su varianza. Se analizaron las deficiencias dentro de la función de De la Mare (1994) y se proporcionaron dos métodos alternativos que pueden respaldar una gama más amplia de valores y de posibles escenarios como, por ejemplo, años de reclutamiento extremadamente bajo.

## Introduction

The Antarctic krill (*Euphausia superba*, hereafter krill) fishery is, by tonnage, the largest fishery in the Southern Ocean (Siegel, 2016). Krill are a key-stone species in the Southern Ocean food web and it is crucial to effectively manage the fisheries to assure its long-term sustainability and conservation (Cavanagh et al., 2021; Kawaguchi and Nicol, 2007; Krumhardt et al., 2022). In 1982, the Commission for the Conservation of Antarctic Marine Living Resources (CCAMLR) was established to conserve Antarctic marine life by, among other things, managing the Southern Ocean fisheries that currently target krill, Patagonian toothfish (*Dissostichus eleginoides*), Antarctic toothfish (*D. mawsoni*) and mackerel icefish (*Champscephalus gunnari*) (Miller, 2011; CCAMLR, 2020). CCAMLR pioneered the use of the ecosystem-based management approach alongside precautionary catch limits to manage their fisheries. This approach works by setting catch limits that take account of the impact of harvesting activities on the ecosystem by ensuring enough biomass of the target species is left to support predators and safeguard healthy breeding populations (Miller, 2011; CCAMLR, 2020). These limits are accompanied by an additional level of precaution known as the ‘trigger’ level, which is equivalent to 1% of the total estimated biomass of krill. The trigger level is set well below the total allowable catch limit as a safeguard measure to allow for uncertainties in future climate and harvesting challenges (Cavanagh et al., 2021; Hill et al., 2016; Parkes, 2000). Understanding the dynamics and impacts of harvesting is essential for selecting appropriate catch limits. This optimisation requires estimates of total abundance, age-specific mortality and recruitment (Constable and de la Mare, 2003; Siegel, 2005). However, collecting these data from field surveys is currently limited in Southern Ocean species due to the extreme and dynamic conditions of the area and the ensuing cost of surveying (Cox et al., 2011; Constable and Kawaguchi, 2018; Kennicutt et al., 2015; Krag et al., 2018). Uncertainties about population parameters for stock assessments led to the development of the generalised yield model (GYM) (Constable and de la Mare, 1996). The GYM was designed to simulate age-structured population projections based on estimated recruitment and mortality parameters from survey data. These projections are then used to explore population scenarios based on current harvesting levels and future harvesting

strategies to establish sustainable catch limits for upcoming harvesting seasons (Constable and de la Mare, 2003; CCAMLR 2020).

Recruitment and mortality are the key drivers of age-structured population projections. In the GYM, these parameters can be simulated using several methods, the most common being the proportional recruitment function (de la Mare, 1994). Traditionally, fisheries rely on estimates of absolute biomass of recruits for stock projections rather than proportional recruitment. Since krill biomass at recruitment is difficult to estimate reliably, de la Mare’s (1994) model uses krill surveys to determine the proportion of recruits seen in a particular age class, to then calculate the properties of the distribution of recruits. De la Mare’s (1994) model aims to reproduce the observed values of the mean proportion of recruits and its variance from the survey by estimating the scaling of natural mortality and the distribution of random recruits (Constable and de la Mare, 2003).

De la Mare’s (1994) proportional recruitment model is a key element of the GYM when used for krill and it is important to evaluate its capacity and further development (SC-CAMLR, 2019). Current environmental threats are enhancing the likelihood and severity of extreme events such as the recurrence of years with low recruitment (Reiss et al., 2008; Kawaguchi et al., 2009). Recruitment is generally accepted to be influenced by extrinsic and intrinsic factors, making it more episodic and not uniform as per the assumptions in models (Quetin and Ross, 2003; Meyer et al., 2020). If periodicity breaks down, which one might expect under the impacts of expected climate change scenarios and increased harvesting pressures, unusual events with consecutive poor recruitment are more likely to occur (Siegel and Loeb, 1995; Quetin and Ross, 2003; Cavanagh, 2021). The increase in the recurrence of years with low recruitment is likely to cause issues when using de la Mare’s (1994) proportional recruitment model (see, for example, Kinzey et al., 2013).

This study explores the properties of the de la Mare (1994) proportional recruitment method and determines its capacity to reproduce the highly variable reproduction scenarios. A more direct derivation that facilitates the simulation of a broader range of scenarios is presented, which also allows for sporadic events of the reoccurrence of

years with low recruitment. These methods are all implemented in the Grym, an open-source package designed to reimplement the GYM and work within R (R Core Team, 2018) (Maschette et al., 2023; Wotherspoon and Maschette, 2020).

## Development of the model

To model recruitment, de la Mare (1994) presents a method that aims to reproduce the mean ( $\hat{\mu}_{\mathfrak{R}}$ ) and variance ( $\hat{\sigma}_{\mathfrak{R}}^2$ ) of the proportion of recruits ( $\mathfrak{R}$ ) observed in the survey data.<sup>1</sup> In the model, de la Mare (1994) assumes that recruitment is independent of the size of the population and that krill in each age class have experienced constant mortality and have all come from a random distribution with constant mean and variance. De la Mare (1994) considers the proportion  $\mathfrak{R}(r)$ , as the ratio of the number of individuals  $A_r$  in age class  $r$  to the number of individuals in that age class or above ( $\sum_{k=r} A_k$ )

$$\mathfrak{R}(r) = \frac{A_r}{\sum_{k=r} A_k}, \quad (1)$$

and proposes a model for recruitment in which the number of recruits to age class  $r$  is a stochastic multiple of the expected number of individuals in all older age classes

$$A_r = \frac{R}{1-R} E\left(\sum_{k=r+1} A_k\right), \quad (2)$$

where  $R$  is a random variable with range [0, 1], and the mean and variance of  $R$  must be chosen in order to reproduce the mean and variance of  $\mathfrak{R}(r)$  observed in survey data. The difficulty with this approach is that as the observed  $\mathfrak{R}(r)$  is a nonlinear function of the random variable  $R$ , it is necessary to apply multiple bias corrections when deriving the mean and variance of  $R$ , making the results difficult to generalise. Specifically, when presented with high variance cases, the model fails to reproduce the properties  $\mathfrak{R}(r)$ . Here, a more direct approach is proposed, that facilitates generalisation of the recruitment model technique to a wide set of distributions.

In the proposed method, the number of recruits to the first age class is a stochastic multiple  $Q$  of the expected number of individuals in all older age classes

$$A_1 = QE\left(\sum_{k=2} A_k\right) \quad (3)$$

In this formulation  $Q$  is a random variable with range [0,  $\infty$ ) and we have assumed the population recruits to the first age class. The mean  $\mu_{\mathfrak{R}}$  and variance  $\sigma_{\mathfrak{R}}^2$  of  $Q$  are again chosen to reproduce  $\hat{\mu}_{\mathfrak{R}}$  and  $\hat{\sigma}_{\mathfrak{R}}^2$  observed in the survey data. Eliminating the ratio  $R/(1-R)$  greatly simplifies the derivation of expressions for  $\mu_Q$  and  $\sigma_Q^2$ .

To derive the model, let  $A_k$  denote the number of individuals currently in age class  $k$ ,  $a_k$  the number of individuals originally recruited to that cohort and  $S_k$  the survival from recruitment to the current year, so that for each age class  $A_k = a_k S_k$ , with  $A_1 = a_1$  and  $S_1 = 1$ . Further, it is required that the survival  $S_k = S_k(M)$  are functions of a common instantaneous mortality  $M$ . For later convenience, the sums are defined as

$$\begin{aligned} s_0 &= \sum_{k=2} S_k, \\ s_1 &= S_r^{-1} \sum_{k=r+1} S_k, \\ s_2 &= S_r^{-2} \sum_{k=r+1} S_k^2. \end{aligned}$$

De la Mare (1994) explains that finding the proportion of recruits essentially translates to finding the rate of natural mortality. While in the de la Mare (1994) derivation  $M$  is constant across time and age classes, in the new formulation  $M$  is constant across the age classes but allowed to vary across time, so that younger age classes can experience higher mortality rates compared to older age classes as per natural conditions. Assuming the  $a_k$  are independently and identically distributed with mean  $\mu_a$  and variance  $\sigma_a^2$ . With these definitions, Equation (3) can be written as  $a_1 = A_1 = Q\mu_a \sum_{k=2} S_k$ , and by using the sums  $a_1 = Q\mu_a s_0$ . Taking expectations of both sides shows that  $\mu_Q$  and the sum of the  $S_k$  are inverses of each other, signifying that the

<sup>1</sup>It is assumed throughout that the survey data has already been corrected for any selectivity bias.

rate at which individuals survive is balanced by the rate at which new individuals are recruited.

$$\mu_Q = s_0^{-1}. \quad (4)$$

The model for the number of recruits can then be reduced to

$$a_1 = \frac{\mu_a}{\mu_Q} Q \quad (5)$$

where  $\mu_Q = s_0^{-1}$  and  $\mu_a$  is a free parameter.

Now consider the mean and variance of  $\mathfrak{R}(r)$ . Although we have the population recruit to the first age class, this age class may not be observable in a survey and so we allow for  $r > 1$  in  $\mathfrak{R}(r)$ . Second-order approximations for the mean and variance of a ratio X/Y are (Stuart and Ord, 1998)

$$\begin{aligned} E\left(\frac{X}{Y}\right) &= \frac{E(X)}{E(Y)} - \\ &\quad \frac{\text{Cov}(X, Y)}{E(Y)^2} + \frac{\text{Var}(Y)E(X)}{E(Y)^3} \\ \text{Var}\left(\frac{X}{Y}\right) &= \frac{E(X)^2}{E(Y)^2} \left[ \frac{\text{Var}(X)}{E(X)^2} - \right. \\ &\quad \left. 2 \frac{\text{Cov}(X, Y)}{E(X)E(Y)} + \frac{\text{Var}(Y)}{E(Y)^2} \right] \end{aligned}$$

From which it follows that:

$$\begin{aligned} \mu_{\mathfrak{R}} &= \frac{E(a_r S_r)}{E\left(\sum_{k=r} a_k S_k\right)} - \\ &\quad \frac{\text{Cov}(a_r S_r, \sum_{k=r} a_k S_k)}{E\left(\sum_{k=r} a_k S_k\right)^2} + \frac{E(a_r S_r)}{E\left(\sum_{k=r} a_k S_k\right)^3} \\ &= \frac{1}{(1+s_1)} + \frac{\sigma_a^2(s_2-s_1)}{\mu_a^2(1+s_1)^3}, \end{aligned}$$

and

$$\begin{aligned} \sigma_{\mathfrak{R}}^2 &= \frac{E(a_r S_r)^2}{E\left(\sum_{k=r} a_k S_k\right)^2} \\ &\quad \left[ \frac{\text{Var}(a_r S_r)}{E(a_r S_r)^2} - 2 \frac{\text{Cov}(a_r S_r, \sum_{k=r} a_k S_k)}{E(a_r S_r)E\left(\sum_{k=r} a_k S_k\right)} + \right. \\ &\quad \left. \frac{\text{Var}\left(\sum_{k=r} a_k S_k\right)}{E\left(\sum_{k=r} a_k S_k\right)^2} \right] \\ &= \frac{\sigma_a^2}{\mu_a^2} (1+s_1)^4. \end{aligned}$$

From these expressions it follows that:

$$\sigma_a^2 = \frac{(1+s_1)^4 \mu_a^2 \sigma_{\mathfrak{R}}^2}{(s_1^2 + s_2)} \quad (6)$$

$$\mu_{\mathfrak{R}} = \frac{1}{(1+s_1)} + \frac{(1+s_1)(s_2-s_1)\sigma_{\mathfrak{R}}^2}{s_1^2 + s_2} \quad (7)$$

From Equation (4), it follows immediately that  $\sigma_Q^2 = \left(\frac{\mu_Q}{\mu_a}\right)^2 \sigma_a^2$ , and Equation (5) can be written as

$$\sigma_Q^2 = \frac{(1+s_1)^4 \sigma_{\mathfrak{R}}^2}{s_0^2 (s_1^2 + s_2)}. \quad (8)$$

Finally, as  $s_1$  and  $s_2$  are functions of natural mortality, given estimates of  $\mu_{\mathfrak{R}}$  and  $\sigma_{\mathfrak{R}}^2$  derived from surveys, Equation (6) can be solved for natural mortality  $M$  and hence  $s_0$ ,  $s_1$  and  $s_2$ . Then, in turn,  $\mu_Q$  and  $\sigma_Q^2$  can be estimated from Equations (4) and (8). Mean recruitment  $\mu_{\mathfrak{R}}$  cannot be estimated from  $\mathfrak{R}(r)$ , and must be estimated independently.

In the de la Mare (1994) formulation,  $R$  must lie in the interval  $[0, 1]$ , and since there are limited distributions for a bounded  $[0, 1]$  range, the formulation focuses on the beta distribution. The great advantage of the new formulation is that it provides a direct relationship between  $\mu_Q$  and  $\sigma_Q^2$ , and  $\mu_{\mathfrak{R}}$  and  $\sigma_{\mathfrak{R}}^2$ , and since the  $Q$  element is bounded by a  $[0, \infty)$  range, any family of distributions with support on the positive half line can be used to generate  $Q$  parameters including the gamma, lognormal, truncated normal and inverse beta families.

In particular, the ‘delta’ or ‘zero inflated’ family (Aitchison, 1955) can also be added to simulate cases of occasional recruitment failure. In this case,  $Q$  is computed as

$$Q = \begin{cases} 0 & u < p \\ Q' & u \leq p \end{cases} \quad (9)$$

where  $u$  is a uniform deviate,  $p$  is the probability of occurrence of low recruitment, and  $Q'$  is again a random deviate from a distribution with support on the positive half line. Expressions for  $\mu_Q$  and  $\sigma_Q^2$  in terms of the mean and variance of  $Q'$  are given by Aitchison (1955).

To demonstrate the validity of their original method, de la Mare (1994) presents a table of simulations. These results are reproduced using the beta, gamma, lognormal and inverse beta distributions (Table 1). The derivation presented here produces very similar results to the de la Mare (1994) values, due to the low coefficient of variation (CV) values chosen for the simulation. The simulations were conducted for 10 000 trials for each distribution for consistency with the de la Mare (1994) results.

These simulations show that when variance is low, any of these distributions are suitable for producing accurate results. However, both the method presented above and the original de la Mare (1994) formulation become increasingly inaccurate as  $\sigma_{\mathfrak{R}}^2$  grows. Both methods rely on Taylor series approximations to the mean and variance of a ratio. But these approximations are only reliable for smaller variances, and so as  $\sigma_{\mathfrak{R}}^2$  grows, the expressions for  $\mu_Q$  and  $\sigma_Q^2$  become increasingly inaccurate and the methods fail to reproduce the target  $\hat{\mu}_{\mathfrak{R}}$  and  $\hat{\sigma}_{\mathfrak{R}}^2$ . The nature of the errors in the approximations of the new formulation are presented in Figure 1. The relative error plots for  $\mu_{\mathfrak{R}}$  and  $\sigma_{\mathfrak{R}}^2$  show there are distinctive differences in the target and simulated mean and variance values in high CV and  $M$  zones, reflective of high-variance scenarios.

For large  $\sigma_{\mathfrak{R}}^2$  the required  $\mu_Q$  and  $\sigma_Q^2$  can be reliably determined by tabulation techniques. First note that natural mortality  $M$  determines the survivals  $S_k = S_k(M)$  and in turn  $\mu_Q$  through Equation (4); so, given  $M$  and  $\sigma_Q^2$ , the corresponding  $\mu_{\mathfrak{R}}$  and  $\sigma_{\mathfrak{R}}^2$  can be determined to arbitrary accuracy by

simulation. This process is used to tabulate the  $\mu_Q$ ,  $\mu_{\mathfrak{R}}$  and  $\sigma_Q^2$  corresponding to a range of  $M$  and  $\sigma_Q^2$  parameters. Given a desired  $\mu_{\mathfrak{R}}$  and  $\sigma_{\mathfrak{R}}^2$ , the corresponding  $M$  (and hence  $\mu_Q$ ) and  $\sigma_Q^2$  are determined from the tabulated values by nearest neighbour interpolation. This tabulation method is conceptually simple but computationally expensive and will not be considered further.

De la Mare (1994) notes that the  $\hat{\mu}_{\mathfrak{R}}$  and  $\hat{\sigma}_{\mathfrak{R}}^2$  are estimates derived from a finite number of surveys and proposes resampling  $\hat{\mu}_{\mathfrak{R}}$  from a normal distribution and  $\hat{\sigma}_{\mathfrak{R}}^2$  from a  $\chi^2$  distribution to account for sampling variation. However, as  $\mathfrak{R}(r)$  is a proportion, its variance is bounded, and resampling a  $\hat{\sigma}_{\mathfrak{R}}^2$  from a  $\chi^2$  distribution can lead to variances that are unrealisable. This is likely to be the cause of the failures reported by Kinzey et al. (2013) when simulating with variances drawn from empirical time series that were larger than those used by de la Mare (1994). Maschette et al. (2020) proposed resampling  $\hat{\mu}_{\mathfrak{R}}$  and  $\hat{\sigma}_{\mathfrak{R}}^2$  by parametric bootstrap. Given observed  $\hat{\mu}_{\mathfrak{R}}$  and  $\hat{\sigma}_{\mathfrak{R}}^2$  derived from  $n$  field surveys, the methods described above are used to simulate new surveys and proportions  $\mathfrak{R}(r)$ , from which a new  $\hat{\mu}_{\mathfrak{R}}$  and  $\hat{\sigma}_{\mathfrak{R}}^2$  are estimated. The resampled  $\hat{\mu}_{\mathfrak{R}}$  and  $\hat{\sigma}_{\mathfrak{R}}^2$  produced in this way are guaranteed to be realisable.

As an alternative to the parametric bootstrap, we propose a constrained simulation method that resamples  $\mu_Q$  and  $\sigma_Q^2$  directly and overcomes the need for tabulation techniques when  $\sigma_{\mathfrak{R}}^2$  is large. Similar to the tabulation method presented above, given  $M$  and  $\sigma_{\mathfrak{R}}^2$ , the method simulates  $n$  new surveys and proportions  $\mathfrak{R}(r)$ , and computes the mean  $\tilde{\mu}_{\mathfrak{R}}$  and variance  $\tilde{\sigma}_{\mathfrak{R}}^2$  of the simulated  $\mathfrak{R}(r)$ . But the sequence of stochastic fractions  $\{Q_i\}$  used in the simulation is generated by inverse probability transform; a sequence  $\{u_i\}$  of random uniform deviates  $u_i \sim U(0, 1)$  is generated, and the sequence  $\{Q_i\}$  is calculated as

$$Q_i = F^{-1}(u_i; \mu_Q, \sigma_Q^2) \quad (10)$$

where  $F^{-1}(u_i; \mu_Q, \sigma_Q^2)$  is the inverse distribution function for a suitable distribution with mean  $\mu_Q$  and variance  $\sigma_Q^2$ . In this way, the discrepancy

$$\begin{aligned} D(M, \sigma_Q^2, \{u_i\}) \\ = (\tilde{\mu}_R - \hat{\mu}_R)^2 + (\tilde{\sigma}_R - \hat{\sigma}_R)^2 \end{aligned} \quad (11)$$

between the observed and simulated  $\mu_R$  and  $\sigma_R^2$  can be viewed as a continuous function of  $M$ ,  $\sigma_Q^2$ , and the sequence of uniform deviates  $\{u_i\}$ . For each resample, the sequence  $\{u_i\}$  is held fixed, and  $M$  and  $\sigma_Q^2$  are estimated by minimising  $D(M, \sigma_Q^2, \{u_i\})$ . This determines an  $M$  (and hence  $\mu_Q$ ) and  $\sigma_Q^2$  for a given sequence of random deviates  $\{u_i\}$  and reproduces the observed  $\hat{\mu}_R$  and  $\hat{\sigma}_R^2$  in simulation. Successive  $M$  and  $\sigma_Q^2$  are drawn by repeating the procedure with different sequences  $\{u_i\}$ . For some pathological sequences  $\{u_i\}$  it will not be possible to reduce the discrepancy  $D(M, \sigma_Q^2, \{u_i\})$  to an acceptable level; this will lead to a large number of values in the sequence  $\{u_i\}$  to produce  $M = 0$ . Such sequences should be discarded, and the process repeated for a new sequence. Figure 2 shows the difference between the sequences which should be used and the ones which should be discarded.

One advantage of this process is that correlated recruitment sequences can be generated by simulating correlated sequences  $\{u_i\}$  of uniform deviates with a Gaussian copula approach (Chung and Zhong, 2001; Xiao, 2016). The sequence  $\{u_i\}$  is generated by first generating a sequence  $\{z_i\}$  of correlated normal deviates  $z_i \sim N(0,1)$  with the desired correlation structure. A probability integral transformation is then used to transform this sequence of correlated normal deviates to a sequence  $\{u_i\}$  of correlated uniform deviates

$$u_i = F(z_i) \quad (12)$$

where  $F$  is the distribution function of the standard normal distribution. The  $\{u_i\}$  and the resulting recruitment sequence will have a similar correlation structure to the original  $\{z_i\}$ .

## Discussion

Current environmental threats caused by climate change (including changes to temperature, ocean circulation patterns and community composition), together with future harvesting pressures are demanding flexibility from the GYM in terms of recruitment variability (Cavanagh et al., 2021;

Krumhardt et al., 2022). Here two separate methods have been developed: a fast set of formulae suitable for modelling low-variance recruitment events and a more computationally expensive procedure capable of modelling high-variance recruitment (Figure 3). Both methods allow for a greater variety of distributions than the original de la Mare (1994) formulation. The more sophisticated of the two methods automatically deals with sampling variation in the survey results and can simulate autocorrelated recruitment.

For small variance, the testing of the new derivation showed success at reproducing  $\mu_R$  and  $\sigma_R^2$  values within a limited range of values. Furthermore, the new derivation gives expressions for inverse beta, lognormal and gamma distributions. At low variability, all three distributions produce broadly the same results, but the exact range depends on the higher order moments of the distributions. This difference in expressions means that subtle differences in the distributions will dictate the range of possible  $\mu_R$  and  $\sigma_R^2$  combinations, giving the new derivation a marginally wider coverage area. However, for extreme variances, derived from low-recruitment events, Taylor series approximations fail using both the de la Mare (1994) recruitment model and the new derivation. For somewhat larger variances, the new derivation can be paired with the delta expressions with varying zero proportions to extend the coverage zones into higher parameter ranges. However, as the variance continues to increase, the delta expressions will also fail. This occurs as Taylor delta methods rely on linear approximations to a nonlinear relationship, so simulations remain limited to certain parameters. High-variance combinations will continue to fall outside the plausible range and the simulations will continue to fail. De la Mare's (1994) recruitment model and the new derivation with the delta expressions fail to reproduce the desired parameters at high variance and are therefore not suitable for extreme scenarios.

The purpose of the GYM is to project possible future population scenarios so that sustainable harvesting levels can be established. If models are not capable of efficiently reproducing real-life scenarios such as the recurrence of low recruitment events, they are ineffective for fishery management purposes. Recruitment modelling needs to be more flexible as well as time efficient so it can efficiently

deal with as broad a range of scenarios as possible, including extreme events that produce large CVs.

The new constrained simulation method resamples  $\mu_Q$  and  $\sigma_Q^2$  given  $\mu_R$  and  $\sigma_R^2$ , and generates a random sequence of  $n$  new surveys and proportions  $\mathfrak{R}(r)$ , so that the mean  $\tilde{\mu}_R$  and variance  $\tilde{\sigma}_R^2$  of the simulated  $\mathfrak{R}(r)$  are an exact replica of the parameters extracted from survey data. Like the bootstrap method proposed by Maschette et al. (2020), whenever a constrained simulation is run, the sequence of random deviates must be maintained. It must be emphasised that when the  $M$  is set too low, the simulation will generate some pathological sequences  $\{u_i\}$  that do not accurately represent the desired  $M$  and CV. In these cases, we suggest discarding such sequences and repeating the process with a new sequence. If the process is repeated and the new sequence  $\{u_i\}$  produces the same discrepancies, it could be indicative of an error in the original  $\mathfrak{R}(r)$  from the surveys. Such situations could arise from the unlikely event that all surveys used to generate  $\hat{\mu}_R$  and  $\hat{\sigma}_R^2$  parameters sampled a total of zero recruits. While this scenario is highly unlikely, it should be emphasised that failed recruitment in the surveys is a general indication of the scarcity of recruits in the samples rather than a complete extinction of an age group in the population. There are still a number of uncertainties about krill recruitment failure and its periodicity for modelling and, while population stability is regulated by the balance of krill survival ( $M$ ) and the rate at which new individuals are recruited, when recruitment is low,  $M$  is reflective of this, otherwise the population would decrease considerably in the models.

## Conclusion

Management of the Southern Ocean fisheries, especially the krill fishery, depends on the GYM and its flexibility to model recruitment considering extreme scenarios such as years of failed recruitment. The results of this study present a new derivation of de la Mare's (1994) recruitment function and an alternative derivation that supports recruitment failure. For low CV values, the new derivation is a fast and precise tool that only requires simple calculations to estimate parameters of  $R$ . For high CV values, a constrained simulation method were developed, which can generate results beyond the range of possible  $\mu_R$  and  $\sigma_R^2$  combinations in both

de la Mare's (1994) recruitment model and the new derivation. Overall, the new derivation as well as the constrained simulation method can be used in the GYM to produce more reliable stock assessments. These adjustments to the GYM could have applications for large-scale fisheries such as the krill fishery as well as smaller scale fisheries with large variations in recruitment.

## References

- Aitchison, J. 1955. On the distribution of a positive random variable having a discrete probability mass at the origin. *J. Am. Stat. Assoc.*, 50: 901–908, doi: <https://doi.org/10.2307/2281175>.
- Cavanagh, R.D., P.N. Trathan, S.L. Hill, J. Melbourne-Thomas, M.P. Meredith, P. Hollyman, B.A. Krafft, M.M.C. Muelbert, E.J. Murphy, M. Sommerkorn, J. Turner and S.M. Grant. 2021. Utilising IPCC assessments to support the ecosystem approach to fisheries management within a warming Southern Ocean. *Marine Policy*, 131 (3): 104589, doi: <https://doi.org/10.1016/j.marpol.2021.104589>.
- CCAMLR. 2020. Krill fisheries: Catch history. <https://www.ccamlr.org/en/fisheries/krill>.
- Chung, K.L. and K. Zhong. 2001. *A course in probability theory*. Academic press, San Diego: 419 pp.
- Constable, A.J. and W.K. de la Mare. 1996. A generalised model for evaluating yield and the long-term status of fish stocks under conditions of uncertainty. *CCAMLR Science*, 3: 31–54.
- Constable, A.J. and W.K. de la Mare. 2003. Generalised yield model, version 5.01b. Australian Antarctic Division, Kingston, Australia.
- Constable, A.J. and S. Kawaguchi. 2018. Modelling growth and reproduction of Antarctic krill, *Euphausia superba*, based on temperature, food and resource allocation amongst life history functions. *ICES J. Mar. Sci.*, 75: 738–750, doi: <https://doi.org/10.1093/icesjms/fsx190>.
- Cox, M.J., D.L. Borchers, D.A. Demer, G.R. Cutter and A.S. Brierley. 2011. Estimating the density of Antarctic krill (*Euphausia superba*) from

- multi-beam echo-sounder observations using distance sampling methods. *J. Roy. Stat. Soc. C*, 60 (2): 301–316.
- de la Mare, W.K. 1994. Modelling krill recruitment. *CCAMLR Science*, 1: 49–54.
- Hill, S.L., A. Atkinson, C. Darby, S. Fielding, B.A. Krafft, O.R. Godø, G. Skaret, P.N. Trathan and J.L. Watkins. 2016. Is current management of the Antarctic krill fishery in the Atlantic sector of the Southern Ocean precautionary? *CCAMLR Science*, 23: 31–51.
- Kawaguchi, S. and S. Nicol. 2007. Learning about Antarctic krill from the fishery. *Ant. Sci.*, 19 (2): 219–230.
- Kawaguchi, S., S. Nicol and A.J. Press. 2009. Direct effects of climate change on the Antarctic krill fishery. *Fish. Manag. Ecol.*, 16: 424–427.
- Kennicutt, M., S. Chown, J. Cassano, D. Liggett, L. Peck, R. Massom and W. Sutherland. 2015. A roadmap for Antarctic and Southern Ocean science for the next two decades and beyond. *Antarct. Sci.*, 27 (1): 3–18.
- Kinzey, D., G. Watters and C.S. Reiss. 2013. Effects of recruitment variability and natural mortality on generalised yield model projections and the CCAMLR decision rules for Antarctic krill. *CCAMLR Science*, 20: 81–96.
- Krag, L.A., B.A. Krafft, A. Engås and B. Herrmann. 2018. Collecting size-selectivity data for Antarctic krill (*Euphausia superba*) with a trawl independent towing rig. *PLOS ONE*, 13 (8): e0202027, doi: <https://doi.org/10.1371/journal.pone.0202027>.
- Krumhardt, K.M., M.C. Long, Z.T. Sylvester and C.M. Petrik. 2022. Climate drivers of Southern Ocean phytoplankton community composition and potential impacts on higher trophic levels. *Front. Mar. Sci.*, 9: 916140, doi: 10.3389/fmars.2022.916140.
- Maschette, D., S. Wotherspoon, C. Pavez, P. Ziegler, S. Thanasskos, K. Reid, S. Kawaguchi, D. Welsford and A. Constable. 2020. Generalised R yield model (Grym). Document SC-CAMLR-39/BG/19. CCAMLR, Hobart, Australia: 27 pp.
- Meyer, B., A. Atkinson, K.S. Bernard, A.S. Brierley, R. Driscoll, S.L. Hill, E. Marschoff, D. Maschette, F.A. Perry, C.S. Reiss, E. Rombolá, G.A. Tarling, S.E. Thorpe, P.N. Trathan, G. Zhu and S. Kawaguchi. 2020. Successful ecosystem-based management of Antarctic krill should address uncertainties in krill recruitment, behaviour and ecological adaptation. *Communications Earth & Environment*, 1: 1–12, doi: 10.138/s43247-020-00026-1.
- Miller, D. 2011. Sustainable Management in the Southern Ocean: CCAMLR Science. In: Arthur Berkman P., M.A. Lang, D.W.H. Walton and O.R. Young (Eds). *Science Diplomacy: Antarctica, Science, and the Governance of International Spaces*. Smithsonian Scholarly Press, Washington, doi: <https://doi.org/10.5479/si.9781935623069.103>.
- Parkes, G. Precautionary fisheries management: the CCAMLR approach. 2000. *Marine Policy*, 24 (2): 83–91.
- Quetin, L.B. and R.M. Ross. 2003. Episodic recruitment in Antarctic krill *Euphausia superba* in the Palmer LTER study region. *Mar. Ecol. Progr. Ser.*, 259: 185–200.
- R Development Core Team. 2018. R: A language and environment for statistical computing. R Foundation for Statistical Computing, Vienna, Austria. [www.R-project.org](http://www.R-project.org).
- Reiss, C.S., A.M. Cossio, V. Loeb and D.A. Demer. 2008. Variations in the biomass of Antarctic krill (*Euphausia superba*) around the South Shetland Islands, 1996–2006. *ICES J. Mar. Sci.*, 65 (4): 497–508, doi: 10.1093/icesjms/fsn033.
- SC-CAMLR. 2019. *Report of the thirty-eighth meeting of the Scientific Committee (SC-CAMLR-38)*. CCAMLR, Hobart, Australia: 433 pp.
- Siegel, V. 2005. Distribution and population dynamics of *Euphausia superba*: Summary of recent findings. *Polar Biol.*, 29: 1–22.
- Siegel, V. 2016. *Biology and Ecology of Antarctic Krill*. AVPE. Springer, Cham, Switzerland.
- Siegel, V. and V. Loeb. 1995. Recruitment of Antarctic krill *Euphausia superba* and possible causes for its variability. *Mar. Ecol. Prog. Ser.*, 123: 45–56.

Stuart, A. and K. Ord. 1998. *Kendall's advanced theory of statistics, distribution theory*. 6th edition. Oxford Univ. Press, New York: 704 pp.

Wotherspoon, S. and D. Maschette. 2020. Grym: R implementation of the generalized yield model. R package version 0.1.0.9000. [github.com/AustralianAntarcticDivision/Grym](https://github.com/AustralianAntarcticDivision/Grym).

Xiao, Q. 2016. Calculating correlation coefficient for Gaussian copula. arXiv e-prints:arXiv: 1608.00738, doi: <https://doi.org/10.48550/arXiv.1608.00738>.

Table 1: Exact outcomes of the 10 000 trials of each distribution for the four target parameters presented in de la Mare (1994).  $\hat{\mu}_{\mathfrak{R}}$ ,  $\hat{\sigma}_{\mathfrak{R}}^2$  and  $\widehat{CV}_{\mathfrak{R}}$  represent the target values of  $\mathfrak{R}$  parameters (highlighted in grey), and  $\mu_{\mathfrak{R}}$ ,  $\sigma_{\mathfrak{R}}^2$  and  $CV_{\mathfrak{R}}$  represent the simulated values generated with the new formulation. The beta distribution results are the same as the ones presented in de la Mare (1994), while the gamma, lognormal and inverse beta results are derived using the new formulation presented in this study. In this procedure, success is measured by the ability of the model to replicate the target  $\hat{\mu}_{\mathfrak{R}}$ ,  $\hat{\sigma}_{\mathfrak{R}}^2$  and  $\widehat{CV}_{\mathfrak{R}}$  values.

Distribution	$\hat{\mu}_{\mathfrak{R}}$	$\mu_{\mathfrak{R}}$	$\hat{\sigma}_{\mathfrak{R}}^2$	$\sigma_{\mathfrak{R}}^2$	$\widehat{CV}_{\mathfrak{R}}$	$CV_{\mathfrak{R}}$
Beta (de la Mare 1994)	0.3	0.300	0.00998	0.011	0.333	0.338
Gamma	0.3	0.300	0.00998	0.009	0.333	0.323
Lognormal	0.3	0.300	0.00998	0.009	0.333	0.310
Inverse beta	0.3	0.300	0.00998	0.009	0.333	0.312
Beta (de la Mare 1994)	0.5	0.499	0.01	0.011	0.2	0.207
Gamma	0.5	0.499	0.01	0.010	0.2	0.195
Lognormal	0.5	0.500	0.01	0.009	0.2	0.188
Inverse beta	0.5	0.500	0.01	0.009	0.2	0.186
Beta (de la Mare 1994)	0.5	0.496	0.02002	0.022	0.283	0.299
Gamma	0.5	0.500	0.02002	0.019	0.283	0.275
Lognormal	0.5	0.500	0.02002	0.016	0.283	0.249
Inverse beta	0.5	0.500	0.02002	0.015	0.283	0.246
Beta (de la Mare 1994)	0.7	0.690	0.01002	0.012	0.143	0.158
Gamma	0.7	0.700	0.01002	0.011	0.143	0.149
Lognormal	0.7	0.700	0.01002	0.009	0.143	0.138
Inverse beta	0.7	0.700	0.01002	0.009	0.143	0.132

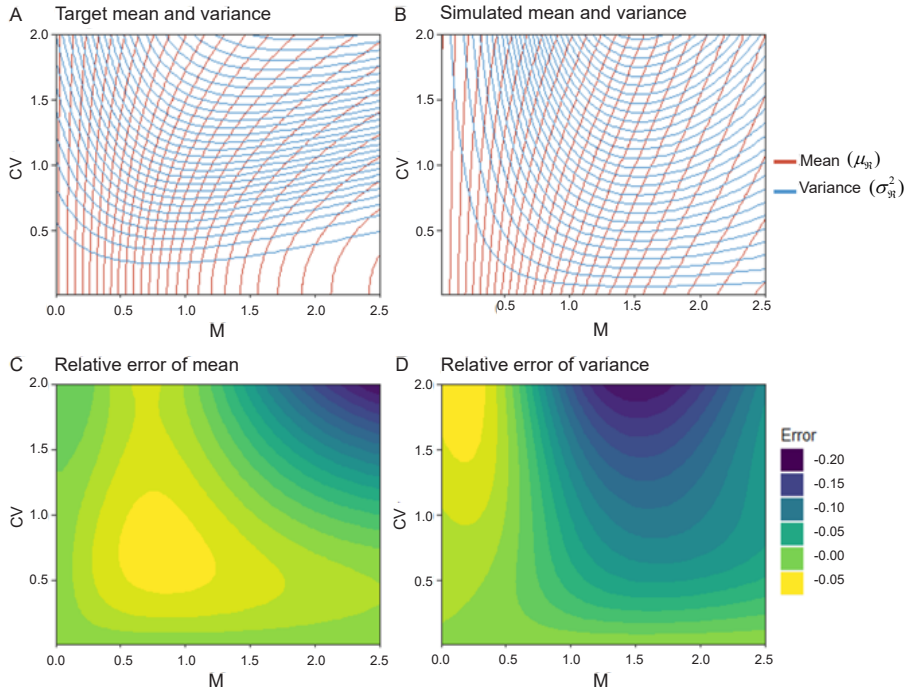


Figure 1: Nature of the errors produced with the new recruitment derivation. (A) Plot of the  $\mu_R$  (red contours) and  $\sigma_{\mathfrak{R}}^2$  (blue contours) of the target CV and M of recruitment. (B) Plot of the simulated  $\mu_R$  (red contours) and  $\sigma_{\mathfrak{R}}^2$  (blue contours) using the recruitment derivation method. The relative errors are presented for the  $\mu_R$  in plot (C), and for the  $\sigma_{\mathfrak{R}}^2$  in plot (D). These high-error regions (blue) are representative of areas where the simulated and  $\sigma_{\mathfrak{R}}^2$  are not accurate reproductions of the target  $\mu_R$  and  $\sigma_{\mathfrak{R}}^2$ .

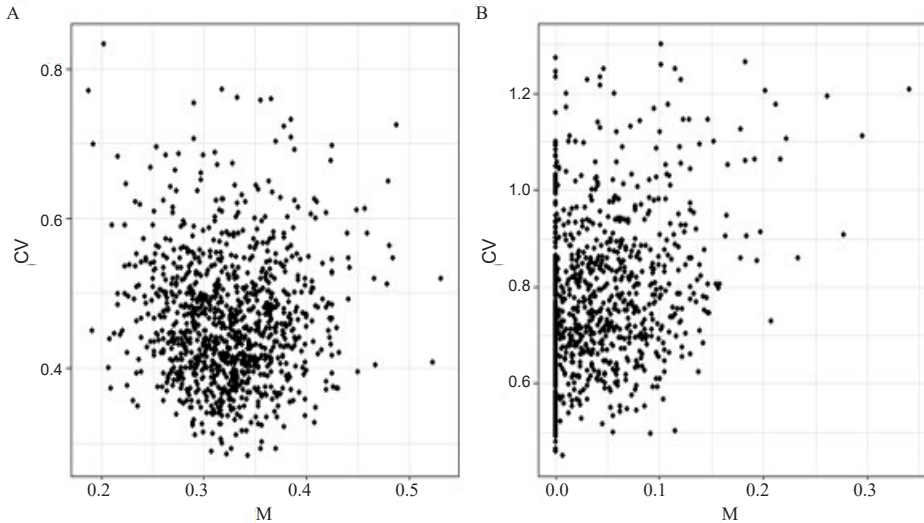


Figure 2: M and CV of target  $\hat{\mu}_{\mathfrak{R}}$  and  $\hat{\sigma}_{\mathfrak{R}}^2$  values generated from a random sequence. (A) Plot derived from parameters used in de la Mare (1994) tests for the gamma distribution assuming target  $\hat{\mu}_{\mathfrak{R}}$  are estimated from 17 surveys. (B) Plot showing the discrepancies generated with parameter from a sequence derived from low  $\hat{\mu}_{\mathfrak{R}}$  values. Failed sequences (B) should be discarded and a new one generated in their place.

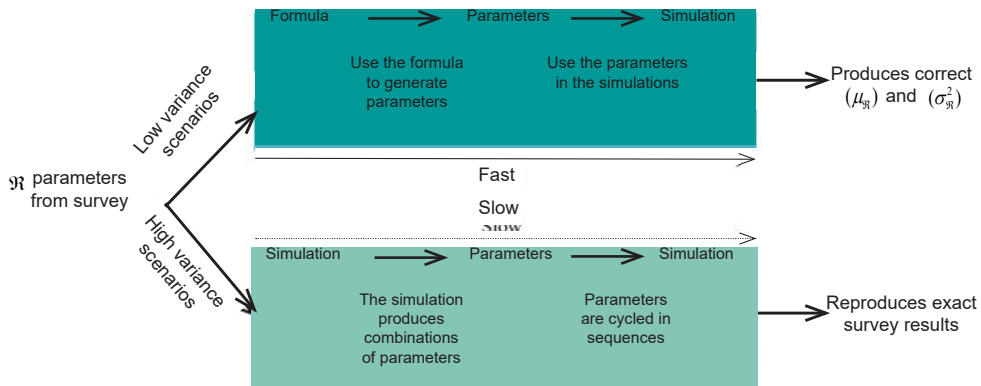


Figure 3: Modelling processes of both methods presented in this study. The CV of from the survey data defines which method should be used. For low-variance scenarios, the formula method (presented in blue) should be used, as it gives fast and precise results. For high-variance scenarios, the simulation method (presented in green) should be used. While the simulation method is very time costly, it is the only modelling process that accurately reproduces the survey parameters in high-variance scenarios.

#### Liste des tableaux

Tableau 1 : Résultats exacts de 10 000 essais de chaque distribution des quatre paramètres cibles présentés dans l'étude de la Mare (1994).  $\hat{\mu}_{\mathfrak{R}}$ ,  $\hat{\sigma}_{\mathfrak{R}}^2$  et  $\widehat{CV}_{\mathfrak{R}}$  représentent les valeurs cibles des paramètres  $\mathfrak{R}$  (surlignés en gris), et  $\mu_{\mathfrak{R}}$ ,  $\sigma_{\mathfrak{R}}^2$  et  $CV_{\mathfrak{R}}$  représentent les valeurs simulées générées grâce à la nouvelle formulation. Les résultats de la distribution bêta correspondent à ceux présentés par de la Mare (1994), alors que les résultats de gamma, lognormaux et de l'inverse d'une distribution bêta sont calculés au moyen de la nouvelle formulation présentée dans cette étude. Lors de cette procédure, le succès est mesuré par la capacité du modèle à reproduire les valeurs cibles  $\hat{\mu}_{\mathfrak{R}}$ ,  $\hat{\sigma}_{\mathfrak{R}}^2$  et  $\widehat{CV}_{\mathfrak{R}}$ .

#### Liste des figures

Figure 1: Nature des erreurs produites avec le nouveau calcul du recrutement. (A) Représentation graphique de  $\mu_R$  (courbes rouges) et  $\sigma_{\mathfrak{R}}^2$  (courbes bleues) du CV cible et de M du recrutement. (B) Représentation graphique de  $\mu_R$  simulé (courbes rouges) et de  $\sigma_{\mathfrak{R}}^2$  (courbes bleues) grâce à la méthode de calcul du recrutement. Les erreurs relatives pour  $\mu_R$  sont présentées sur le graphique (C) et pour  $\sigma_{\mathfrak{R}}^2$  sur le graphique (D). Ces régions à fort taux d'erreur (en bleu) sont représentatives des aires où  $\mu_R$  et  $\sigma_{\mathfrak{R}}^2$  simulés ne reproduisent pas  $\mu_R$  et  $\sigma_{\mathfrak{R}}^2$  cibles correctement.

Figure 2 : M et CV des valeurs  $\hat{\mu}_{\mathfrak{R}}$  et  $\hat{\sigma}_{\mathfrak{R}}^2$  cibles générées à partir d'une séquence aléatoire. (A) Représentation graphique du calcul des paramètres utilisés dans les tests de de la Mare (1994) pour la distribution de gamma en présupposant que les valeurs cibles  $\hat{\mu}_{\mathfrak{R}}$  sont estimées à partir de 17 campagnes d'évaluation. (B) Représentation graphique des incohérences générées avec le paramètre d'une séquence calculé à partir de faibles valeurs de  $\hat{\mu}_{\mathfrak{R}}$ . Les séquences non fructueuses (B) devraient être retirées et remplacées par de nouvelles séquences.

Figure 3 : Processus de modélisation des deux méthodes présentées dans cette étude. Le CV de  $\mathfrak{R}(r)$  issu des données de la campagne d'évaluation définit la méthode qui devrait être utilisée. Dans les scénarios de faible variance, la méthode basée sur une formule (représentée en bleu) devrait être utilisée, car elle donne des résultats rapides et précis. Dans les scénarios de variance élevée, la méthode basée sur une simulation (représentée en vert) devrait être utilisée. Bien que la méthode basée sur une simulation prenne bien plus de temps, elle constitue le seul processus de modélisation qui reproduise correctement les paramètres d'une campagne d'évaluation dans des scénarios de variance élevée.

## Список таблиц

Таблица 1: Точные результаты 10 000 испытаний каждого распределения для всех четырех целевых параметров, которые были представлены в исследовании де ла Маре (1994). Значения  $\hat{\mu}_R$ ,  $\hat{\sigma}_R^2$  и  $\widehat{CV}_R$  (выделенные серым цветом) представляют собой целевые значения параметров  $\Re$ , а  $\mu_R$ ,  $\sigma_R^2$  и  $CV_R$  представляют собой смоделированные значения, полученные с помощью новой формулировки. Результаты бета-распределения совпадают с результатами, представленными в работе Де Ла Маре (1994), в то время как результаты гамма-, логнормального и обратного бета-распределения были получены с использованием новой формулировки, представленной в данном исследовании. В данном процессе успех измеряется способностью модели воспроизвести целевые показатели  $\hat{\mu}_R$ ,  $\hat{\sigma}_R^2$  и значения  $\widehat{CV}_R$ .

## Список рисунков

Рис. 1: Характер ошибок, возникающих в результате использования нового метода пополнения. (A) График  $\mu_R$  (красный контур) и  $\sigma_R^2$  (синий контур) целевых значений CV и M пополнения. (B) График смоделированного  $\mu_R$  (красный контур) и  $\sigma_R^2$  (синий контур) с использованием метода вычисления пополнения. Относительные ошибки для  $\mu_R$  представлены на графике (C), а для  $\sigma_R^2$  на графике (D). Данные области с высокой погрешностью (синие) представляют собой смоделированные показатели  $\mu_R$  и  $\sigma_R^2$ , и не являются точным отражением целевых показателей  $\mu_R$  и  $\sigma_R^2$ .

Рис. 2: Целевые значения  $M$  и  $CV$  для  $\hat{\mu}_R$  и  $\hat{\sigma}_R^2$  полученные на основе случайной последовательности. (A) График, построенный на основе параметров, использованных в анализах Де Ла Маре (1994) для гамма-распределения, при условии, что целевые показатели  $\hat{\mu}_R$  оцениваются по результатам 17 съемок. (B) График, показывающий расхождения, возникающие при использовании параметров последовательности, полученной из низких значений  $\hat{\mu}_R$ . Последовательности, не давшие результата (B), должны быть исключены, а на их месте составлены новые.

Рис. 3: Процессы моделирования обоих методов, представленных в данном исследовании. Значение  $CV$  для  $\Re(r)$  по данным съемок позволяет определить, какой метод следует использовать. Для сценариев с низкой дисперсией следует использовать метод расчета по формуле (представленный синим цветом), так как он дает быстрые и точные результаты. Для сценариев с высокой степенью вариативности следует использовать метод расчета с помощью моделирования (выделен зеленым цветом). Несмотря на то, что метод моделирования требует больших временных затрат, он является единственным средством моделирования, которое точно воспроизводит параметры съемки в сценариях с высокой вариативностью.

## Lista de las tablas

Tabla 1: Resultados exactos de las 10 000 pruebas de cada distribución para los cuatro parámetros objetivos presentados en De la Mare (1994).  $\hat{\mu}_R$ ,  $\hat{\sigma}_R^2$   $\widehat{CV}_R$  representan los valores objetivos de los parámetros  $\Re$  (resaltados en gris), mientras que  $\mu_R$ ,  $\sigma_R^2$  y  $CV_R$  representan los valores simulados generados con la nueva formulación. Los resultados de la distribución beta son los mismos que los presentados en De la Mare (1994), mientras que los resultados de las distribuciones gamma, lognormal e inversa beta se derivan utilizando la nueva formulación presentada en este estudio. En este procedimiento, el éxito se mide por la capacidad del modelo para replicar los valores objetivos de  $\hat{\mu}_R$ ,  $\hat{\sigma}_R^2$  y  $\widehat{CV}_R$ .

## Lista de las figuras

Figura 1: Naturaleza de los errores producidos con la nueva derivación de reclutamiento. (A) Gráfico de  $\mu_R$  (cotas en rojo) y de  $\sigma_R^2$  (cotas en azul) para el CV y la  $M$  objetivo del reclutamiento. (B) Gráfico de  $\mu_R$  (cotas en rojo) y de  $\sigma_R^2$  (cotas en azul) para la simulación del CV y de la  $M$  utilizando el método de derivación de reclutamiento. Los errores relativos se presentan para  $\mu_R$  el gráfico (C), y para  $\sigma_R^2$  en el gráfico (D). Estas regiones con altos niveles de error (azul) son representativas de áreas donde las simulaciones de  $\mu_R$  y  $\sigma_R^2$  no son reproducciones precisas de los valores objetivo  $\mu_R$  y  $\sigma_R^2$ .

Figura 2:  $M$  y CV de los valores objetivo  $\hat{\mu}_{\mathfrak{R}}$  y  $\hat{\sigma}_{\mathfrak{R}}^2$  generados a partir de una secuencia aleatoria. Las secuencias fallidas (B) deben descartarse y generarse una nueva en su lugar. (A) Gráfico derivado de parámetros utilizados en las pruebas de De la Mare (1994) para la distribución gamma, asumiendo que los valores objetivo  $\hat{\mu}_{\mathfrak{R}}$  se estiman a partir de 17 prospecciones. (B) Gráfico que muestra las discrepancias generadas con parámetros de una secuencia derivada de valores bajos de  $\hat{\mu}_{\mathfrak{R}}$ . Las secuencias fallidas (B) deben descartarse y, en su lugar, deberían generarse nuevas secuencias.

Figura 3: Mecanismos de modelado de ambos métodos presentados en este estudio. El CV de  $\mathfrak{R}(r)$  a partir de los datos de la prospección define qué método debe utilizarse. Para escenarios de baja varianza, se debe utilizar el método de fórmula (presentado en azul), ya que proporciona resultados rápidos y precisos. Para escenarios de alta varianza, se debe utilizar el método de simulación (presentado en verde). Aunque el método de simulación requiere de una gran cantidad de tiempo, es el único proceso de modelado que reproduce con precisión los parámetros de la prospección en escenarios de alta varianza.

## APPENDIX 1

## List of equation terms

Model parameters	Description
$(\mathfrak{R})$	Proportion of recruits observed in survey data
$\hat{\mu}_{\mathfrak{R}}$	Mean of the proportion of recruits observed in survey data
$\hat{\sigma}_{\mathfrak{R}}^2$	Variance of the proportion of recruits observed in survey data
$\widehat{CV}_{\mathfrak{R}}$	Coefficient of variation observed in survey data
$\mu_{\mathfrak{R}}$	Simulated mean of the proportion of recruits
$\sigma_{\mathfrak{R}}^2$	Simulated variance of the proportion of recruits
$CV_{\mathfrak{R}}$	Simulated coefficient of variation
$r$	The first age class observed in the survey data
$A$	The number of individuals in a given age class observed in the survey data
$A_k$	The number of individuals in every age class observed in the survey data
$R$	Random variable used in the stochastic fraction
$A_1$	Number of recruits to the first age class
$Q$	Random variable that replaces the stochastic fraction
$\mu_Q$	Mean of $Q$
$\sigma_Q^2$	Variance of $Q$
$a$	The number of individuals originally recruited to an age class
$\mu_a$	Mean of $a$
$\sigma_a^2$	Variance of $a$
$S_k$	Survival from recruitment to the observed age class in the survey data
$M$	Instantaneous mortality
$Q'$	A random variable that supports the delta expression
$u$	Uniform deviate used in the delta expression
$p$	Probability of occurrence of low recruitment used in the delta expression